ACS Partner Journal

ACCOUNTS
—of materials research—

pubs.acs.org/amrcda

Article

Coordination and Architecture Regulation of Electrocatalysts for Sustainable Hydrogen Energy Conversion

Miao-miao Shi, Di Bao, Jun-min Yan, Hai-xia Zhong,* and Xin-bo Zhang*

Cite This: *Acc. Mater. Res.* 2024, 5, 160−172

Read Online

ACCESS | Metrics & More | Article Recommendations

CONSPECTUS: With the increasing concerns about the energy and environmental crisis, hydrogen, with the high energy density and cleanliness, has been widely regarded as one ideal energy carrier for adjusting the fossil fuel dependent energy system. In this context, extensive studies are focused on improving the efficiency of the sustainable hydrogen production, storage, and utilization coupled with the renewable energy. And it can be realized in electrolysis cells and fuel cell devices. Several electrochemical reactions are involved, such as water splitting (hydrogen/oxygen evolution: HER/OER) for hydrogen production, electroreduction of nitrogen/nitrate, and carbon dioxide to NH_3 and HCOOH (NRR, NO_3RR, CO_2RR) for hydrogen storage, and oxygen reduction reaction (ORR) for hydrogen utilization. However, the achieved efficiency of the hydrogen energy conversion is still unsatisfactory due to these intrinsically sluggish electrochemical reactions, which has spawned a revival of research interests in developing the electrocatalysts with high activity, selectivity, and durability. Therefore, various strategies have been established to construct effective electrocatalysts, such as coordination or architecture structure regulation, which will determine the intrinsic activity and the efficiency of mass transport, respectively. Besides, combined with the progress of characterization techniques and theoretical studies, insightful understanding of the electrocatalytic sites and reaction mechanism are also investigated, guiding the rational design of future electrocatalysts.

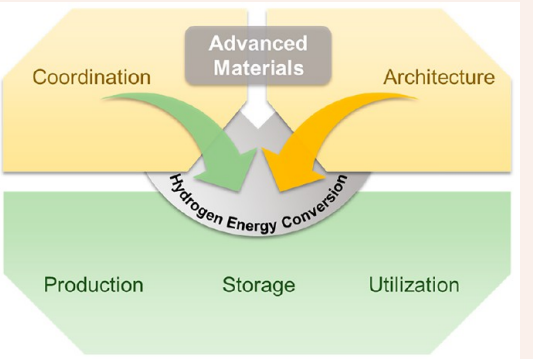

In this Account, we summarize our recent efforts in exploring electrocatalysts through the regulation of coordination and construction of porous architecture structures toward the highly efficient electrochemical hydrogen energy conversion. First, an overview of the hydrogen energy conversion process is presented to reveal the advantages and challenges of these reactions. Then, we introduced effective strategies to optimize the coordination and architecture structure to enhance the catalytic performance, such as tailoring the particle size, valence state, and crystal plane, defect engineering, substrate incorporation, structural reconstruction, etc. Additionally, it is also illustrated the insightful mechanism study on the improvement of the catalytic performance via the experimental characterization and theoretical calculations. Finally, a brief outlook is proposed to address the challenges to be overcome for improving the hydrogen conversion efficiency through developing rational catalysts.

1. INTRODUCTION

Hydrogen (H_2) energy has been widely researched and explored due to its cleanliness and zero carbon emissions with the growing global concern over environmental issues. Another advantage of H_2 energy is its high energy density (120 MJ/kg), which is much higher than that of traditional fuels such as gasoline (46 MJ/kg) and coal (20−30 MJ/kg).[1−3] Due to these advantages, H_2 energy can be widely applied as one of the most prominent clean energy carriers in the fields of transportation, electricity, industry, etc. However, the production, storage, and utilization of H_2 still face technical and economic challenges.

Traditional H_2 production is extracted from natural gas, which demands large amounts of energy, complex equipment, and thus high costs. Electrochemical water splitting, which undergoes through the cathodic hydrogen evolution reaction (HER) and anodic oxygen evolution reaction (OER), has been reported as a promising alternative for H_2 production.[4] Whereas the sluggish reaction dynamics induce the large overpotential and high energy consumption, and thus restrict the wide practical application. For H_2 energy conversion, the storage of H_2 is also very important, which faces great challenges including the refractory to liquefaction and high demands on the tank materials, as well as unsafety problems during transportation. Therefore, extensive endeavors are contributed to exploring the suitable hydrogen storage

Received: September 24, 2023
Revised: November 6, 2023
Accepted: December 18, 2023
Published: January 17, 2024

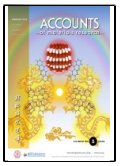

materials, such as formic acid (HCOOH) and ammonia (NH_3), which both possess the considerable hydrogen storage capacity (4.4 and 17.6 wt %). Recently, the electrochemical methods driven by the renewable electricity under ambient conditions are widely investigated for synthesizing HCOOH and NH_3, such as electrochemical carbon dioxide (CO_2), nitrogen (N_2), and nitrate (NO_3^-) reduction. However, the selectivity and yield rate for HCOOH and NH_3 production are unsatisfactory owing to the rapid competitive side reaction and the sluggish target reaction. Regarding the utilization of H_2, fuel cell represents one appealing choice for the conversion of H_2 energy into electrical energy. Fast oxygen reduction reaction (ORR) can efficiently optimize the energy conversion output. Thus, boosting the electrocatalytic reactions can effectively enable the sustainable development of H_2 production, storage, and utilization.

Scheme 1. Illustration of Hydrogen Energy Conversion

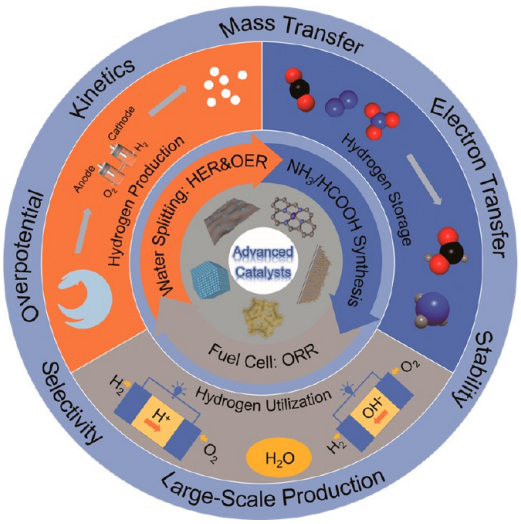

Over these decades, considerable progress in the development of highly active catalysts has been achieved.[5] It was found that the modulation of coordination structure will alter the distribution of electron density and affect the interaction of absorbents on the active site.[6,7] Generally, the intrinsic activity of electrocatalysts is largely influenced by their coordination structure, while the mass transport capacity can be tailored by the porous architecture, which synergistically determines the overall catalytic performance. The three-dimensional (3D) structure can facilitate the transfer of H_2, O_2, N_2, and NO_3^- species. The integrated electrode not only accelerates the charge transfer but also improves the stability. Therefore, through the regulation of coordination and architecture structure, these developed catalytic systems can efficiently promote the electrochemical reactions for hydrogen energy conversion.

In this Account, we aim to summarize our efforts in the regulation of the coordination and architecture structure of the catalysts for the rapid hydrogen energy conversion process, including production (water splitting: HER and OER), storage (NH_3 and HCOOH synthesis), and utilization (fuel cell: ORR). Typical strategies that are proposed to improve the activity of catalysts, and how these strategies adjust the electronic and morphological structure are also illustrated. Finally, we present aspects in the study of catalysts that are deficient and propose an outlook toward the high-efficiency hydrogen energy conversion.

2. PRODUCTION OF HYDROGEN: WATER SPLITTING

2.1. Fundament for Water Splitting

Electrochemical water splitting undergoes via cathodic HER (Acidic electrolyte: $4H^+ + 4e^- \rightarrow 2H_2$, Alkaline electrolyte: $4H_2O + 4e^- \rightarrow 2H_2 + 4OH^-$ $E^\theta = 0$ V vs RHE) and anodic OER (Acidic electrolyte: $2H_2O \rightarrow O_2 + 4H^+ + 4e^-$, Alkaline electrolyte: $4OH^- \rightarrow O_2 + 2H_2O + 4e^-$ $E^\theta = 1.23$ V vs RHE). Due to the slow reaction kinetics, efficient catalysts are urgently needed to enhance the efficiency of H_2 production.[8] For HER, a two-electron transfer process occurs with the Volmer–Heyrovsky or the Volmer–Tafel mechanism.[9] And the performance of the catalysts is largely relevant to the hydrogen adsorption free energy (ΔG_H). Too strong hydrogen adsorption may block the active sites and lead to the failure of H_2 release, while too weak hydrogen adsorption may be unable to form H_2 gas.[10] Pt-based electrocatalysts exhibit great potential due to the moderate ΔG_H which approaches zero, whereas the low reserves and high costs seriously restrict the scale application. For OER, adsorbate evolving mechanism (AEM) and the lattice oxygen mechanism (LOM) pathways are proposed. In comparison with AEM, catalysts working via LOM show better activity but poor stability.[11] Besides, OER is involved in a complex process along with multi-intermediates, such as O*, OH*, and OOH*, which results in sluggish kinetics and large overpotential.[12] Noble metal oxides, especially iridium oxide (IrO_2) and ruthenium oxide (RuO_2), have demonstrated promising activity but are also limited by their high price.[13,14] Therefore, intensive research is focused on non-noble metal catalysts with low cost and high activity.

Generally, principles for constructing the highly efficient catalysts toward electrochemical water splitting mainly focus on the enhancement of intrinsic catalytic activity, the number of active sites, the efficiency of electron and mass transfer, and stability. The intrinsic activity can be regulated by the composition and the electronic structure, which influence the adsorption energy and determine the energy barrier of the key steps. Besides, downsizing the catalysts and enlarging the surface area are usual strategies for increasing the number of active sites. For improving the overall energy efficiency, the 3D porous integrated electrode is widely developed as it can accelerate the transfer of electrons, H^+, OH^-, and H_2O, and promote the desorption of H_2, O_2, as well as stabilize the integrated active species. To evaluate the HER and OER catalysts, several parameters are crucial, such as the overpotential (η) at a certain current density, the Tafel slope, stability, and faradaic efficiency (FE), which are separately associated with the catalytic activity, kinetics, stability, and selectivity.[15] Therefore, several effective strategies are discussed with reference to these key principles.

2.2. Catalysts for HER

Carbon-based materials that possess tunable molecular structures and strong tolerance to acidic/alkaline environments have been widely studied as HER electrocatalysts. And their catalytic performance of HER is associated with the electronic/chemical properties, which can be modified by the architecture of catalysts, such as the reduction in size and introduction of highly conductive substrates, etc. For example, Qiao et al. proposed that the combination of graphitic-carbon nitride (g-C_3N_4) on nitrogen-doped graphene (NG) substrate can realize

https://doi.org/10.1021/accountsmr.3c00197
Acc. Mater. Res. 2024, 5, 160–172

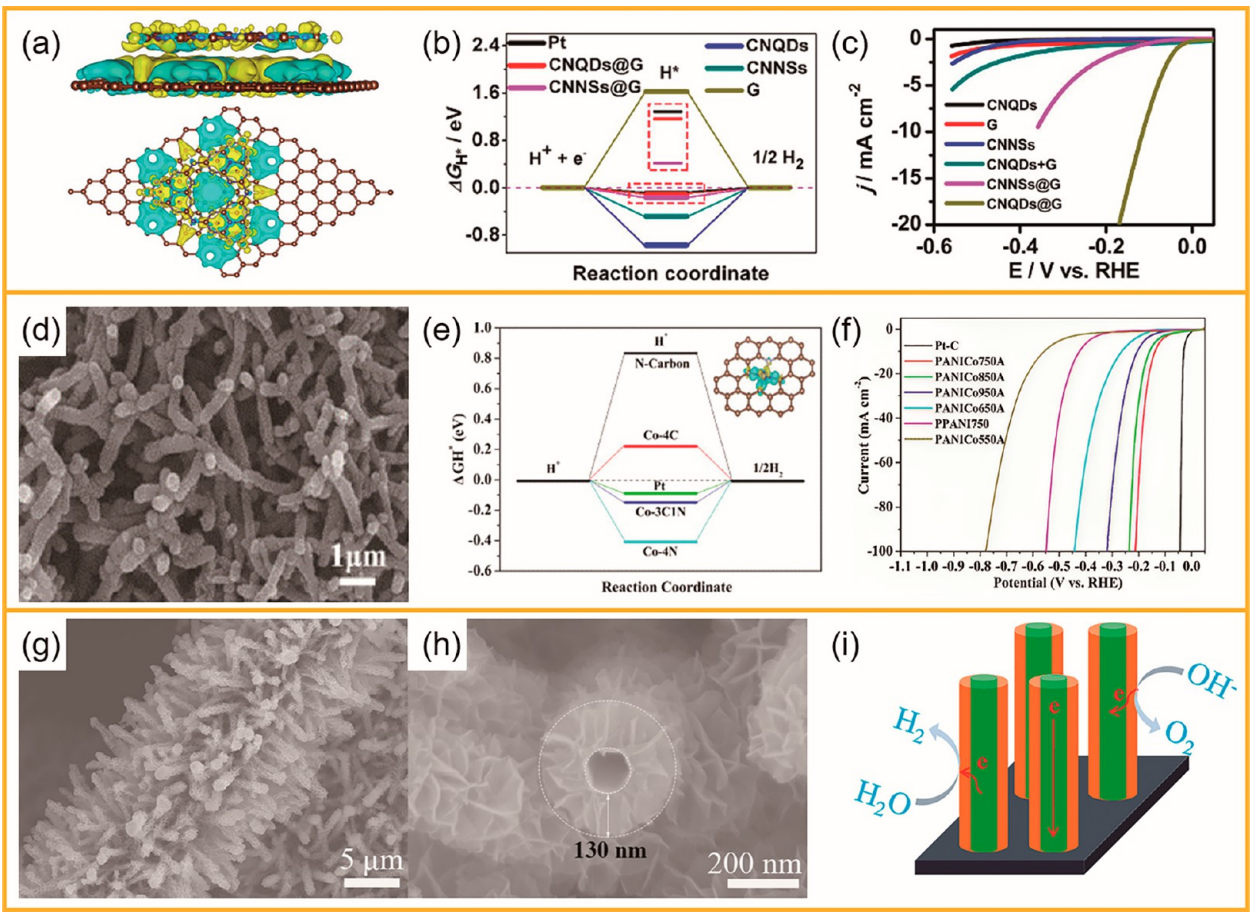

Figure 1. (a) Interfacial electron transfer in CNQDs@G. (d) Schematic structure of CNQDs@G. (c) Free energy diagrams for HER at the equilibrium potentials of CNQDs@G. Reproduced with permission from ref 17. Copyright 2018 American Chemical Society. XANES (d) and EXAFS (e) spectra of Co−C−N. (f) Calculated free-energy diagram of HER at the equilibrium potential of Co−C−N. Reproduced with permission from ref 22. Copyright 2015 American Chemical Society. (g−h) The morphology of 3D CP/CTs/Co−S. (i) Illustration of the gas release and electron transport of CP/CTs/Co−S. Reproduced with permission from ref 23. Copyright 2016 American Chemical Society.

excellent HER activity with a low overpotential of 240 mV at 10 mA cm^{-2} due to the synergistic effect in the promotion of proton adsorption and reaction kinetics.[16] Differently, we improved the HER performance by downsizing the carbon nitrides into the g-C_3N_4 quantum dots (CNQDs) with rich exposed active sites and supporting them on graphene (CNQDs@G) for sufficient electron transfer.[17] CNQDs are active sites that can redistribute the charge density in the interlayer, and reduce the Gibbs free energy of the intermediate state (ΔG_H^*) of 0.1 eV toward fast kinetics, which is close to that of the state-of-the-art Pt catalyst (0.09 eV, Figure 1a, b). As a result, CNQDs@G displays low overpotential (110 mV) at 10 mA cm^{-2}, which is even comparable to many metallic catalysts (Figure 1c). This work emphasizes the importance of quantization and substrate in the synergistic optimization of electronic structure and creation of abundant active sites, withdrawing efficient material design strategy.

In addition, the doping of transition metal atoms and heteroatoms (N, P, S) can also adjust the coordination structure and modulate the electronic state of catalysts as well, then affecting the adsorption of key intermediates.[18,19] Guo et al. demonstrated that the doping of N can create electron-rich environment, and lower the C−H bond energy to stabilize the H* on the surface of catalyst, thereby enhancing the HER activity of N doped carbon electrocatalysts.[20] Besides, metal−nitrogen−carbon (M−N−C) catalysts with low usage of metal atoms have exhibited high catalytic activity.[21] Considering the advantages of high active Co sites and the porous free-standing electrode, a three-dimensional (3D) porous Co−C−N electrode (PANICo) is constructed via four steps: electrodeposition, ions adsorption, carbonization, and acid wash treatment (Figure 1d).[22] X-ray absorption near-edge structure (XANES) and extended X-ray absorption fine structure (EXAFS), density functional theory (DFT) studies reveal the 3C1N hybrid coordination structure with Co−C and Co−N bonds possess a high density of state over the Fermi level and thereby enable the enhanced electron transfer capacity. Additionally, this structure demonstrated a moderate adsorption free energy for H (ΔG_H^*), which is much better than that of Co-4C and Co-4N (Figure 1e). As a result, this PANICo catalyst shows good HER performance with low overpotential (212 mV at 100 mA cm^{-2}) (Figure 1f). Besides the coordination structure, building the 3D integrated structure also works for the enhancement of HER owing to the fast mass and charge transfer. For instance, the integrated 3D carbon paper/carbon tubes/cobalt-sulfide sheets (CP/CTs/Co−S) fabricated by the template-assisted method via well-aligned ZnO nanowires provided a continuous pathway for the rapid

https://doi.org/10.1021/accountsmr.3c00197
Acc. Mater. Res. 2024, 5, 160−172

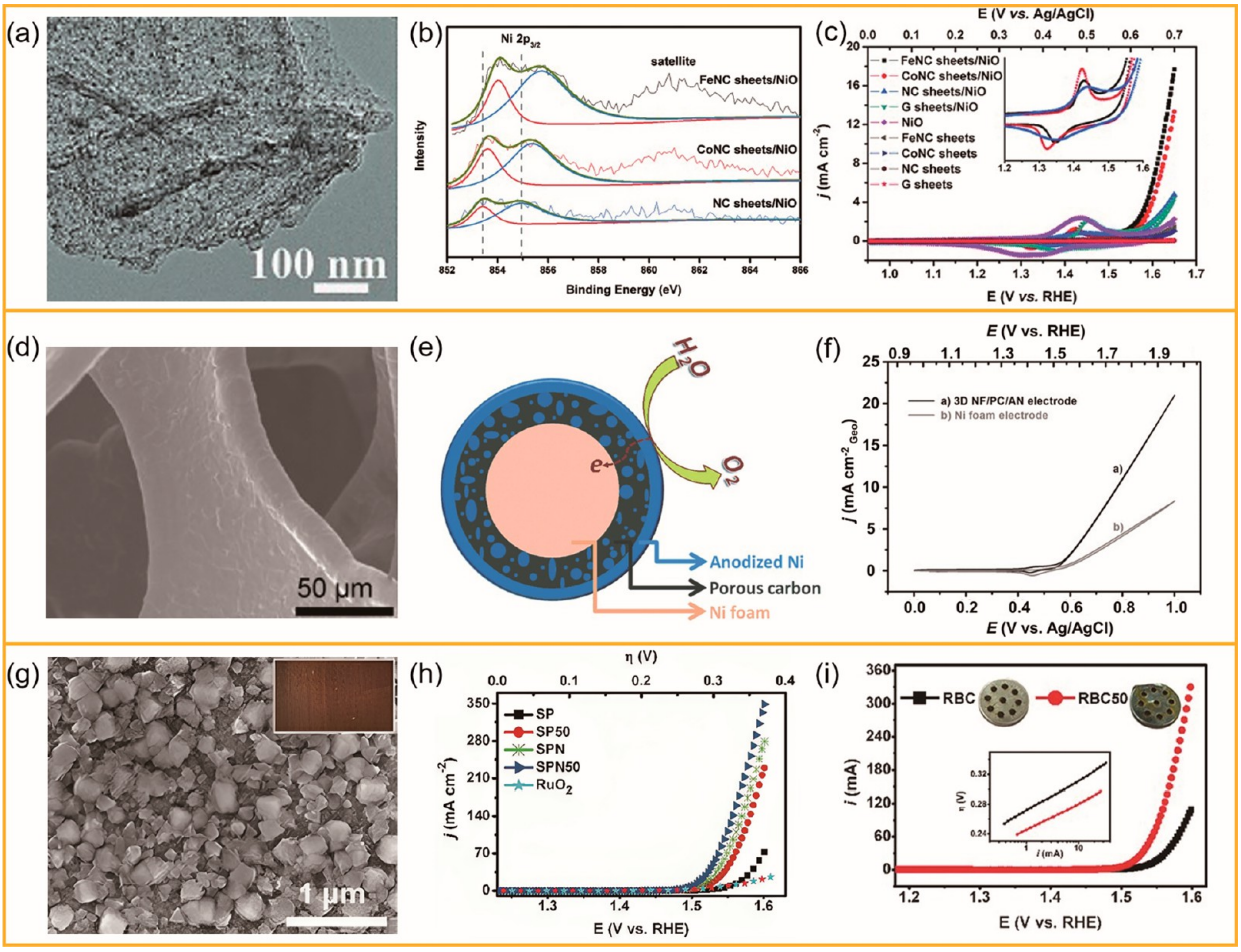

Figure 2. (a) TEM image of FeNC sheets/NiO. (b) High resolution of Ni $2p_{3/2}$ XPS spectra of NiO NPs supported on different substrates. (c) Cyclic voltammetry (CV) curves of OER for different catalysts. Reproduced with permission from ref 25. Copyright 2015 Wiley-VCH. (d) SEM image of the 3D NF/PC/AN electrode. (e) Scheme of 3D NF/PC/AN electrode for OER. (f) CV curves of 3D NF/PC/AN and Ni foam electrode. Reproduced with permission from ref 27. Copyright 2013 Wiley-VCH. (g) SEM image of EORC-activated rusty SS plate, and its corresponding photograph (inset). (h) OER polarization curves of SS plate and corroded stainless steel plate without (SP, SPN) or with (SP50, SPN50) EORC. (i) OER polarization curves of rusty battery case (RBC) before and after EORC. Reproduced with permission from ref 30. Copyright 2016 Wiley-VCH.

electron transport and the gas bubbles release (Figure 1g–i), and exhibited a Tafel slope of 131 mV dec^{-1}.[23]

2.3. Catalysts for OER

Despite the optimization of size, composition, and crystal structure of the active composites of the OER electrocatalysts, the interaction between the active components and the substrate would also affect the catalytic activity.[24] We found that porous metal–nitrogen–carbon (FeNC, CoNC) nanosheets could serve as the appropriate substrate to load active NiO with even dispersion (Figure 2a).[25] The constructed porous NC architecture endows large surface area for rich active sites and simultaneously facilitates mass diffusion. More importantly, the FeNC support can modulate the electronic structure of NiO, as can be seen from the X-ray photoelectron spectroscopy (XPS) data that the binding energies of NiO/FeNC shift positively in comparison with NiO/NC and NiO/CoNC. FeNC sheets possess stronger electron coupling effect (Figure 2b). The electron donation from NiO to FeNC sheets increases the acidity of Ni active sites, which can enhance the interaction between OH^- and NiO NPs according to the Lewis acid–base concept and thus improve the OER activity. Impressively, NiO/FeNC exhibits a low OER onset potential of 1.47 V vs RHE, low overpotential of 0.39 V at 10 mA cm^{-2}, and small Tafel slope of 76 mV/dec (Figure 2c). Compared to the two-dimensional (2D) porous structure, 3D porous architecture is more conducive to improving the electrochemical surface area for exposing more active sites. Ni foam is an ideal candidate owing to its 3D porous structure and high electron conductivity.[26] A 3D Ni foam/porous carbon/anodized Ni (NF/PC/AN) was constructed via the calcination of Ni foam/ZIF-8 followed by acid etching and electrochemical anodization treatment to promote the OER process, wherein porous carbon is derived from ZIF-8 (Figure 2d).[27] After the anodization, the active component of γ-NiOOH is generated on 3D NF/PC/AN electrode (Figure 2e). Differently, the Ni foam shows NiO and $Ni(OH)_2$ species after anodization, which is easily dehydrated to deactivation without the protective carbon layer. Therefore, this strategy not only enhances the activity but also increases the stability of OER electrocatalysts (Figure 2f).

Besides Ni foam, stainless steel (SS) also displays enormous potential for 3D integrated OER electrode because of the good electron conductivity and the existence of rich active elements (Fe, Ni, and Mn).[28] A hierarchical cross-linked Ni(Fe)

https://doi.org/10.1021/accountsmr.3c00197
Acc. Mater. Res. 2024, 5, 160–172

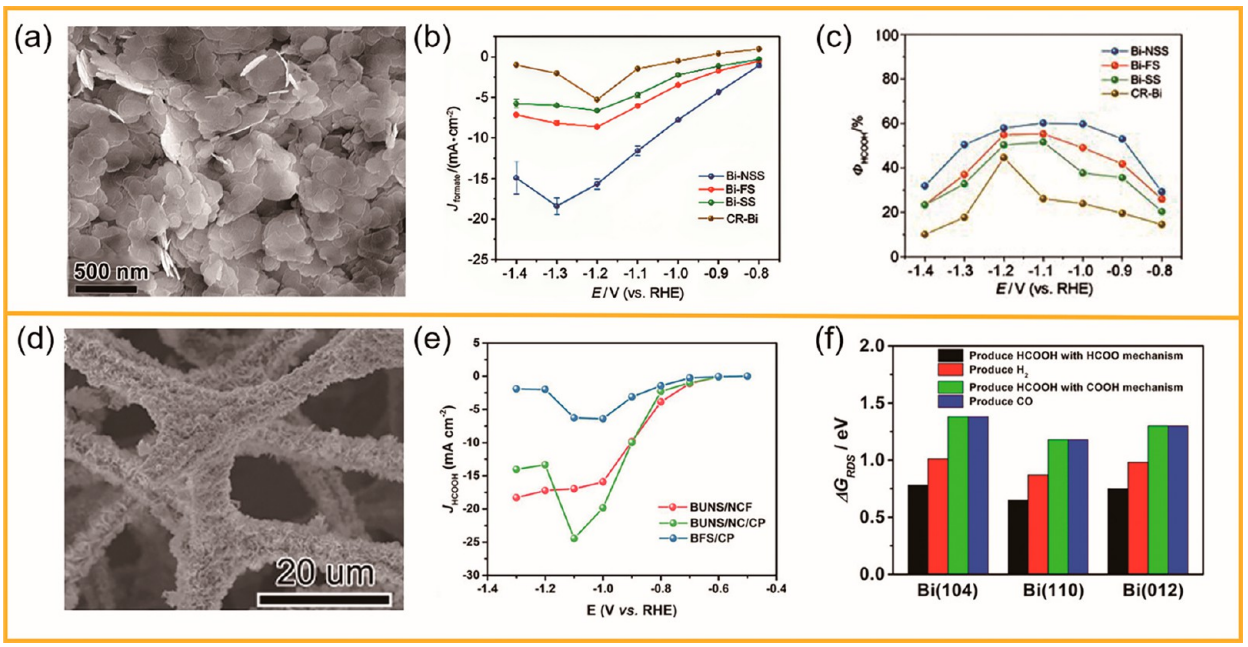

Figure 3. (a) SEM image of Bi-NSS. (b) Partial current densities for HCOOH production at different potentials. (c) Cathodic energy efficiency of Bi based catalysts at different potentials. Reproduced with permission from ref 34. Copyright 2020 Wiley-VCH. (d) SEM image of BUNS/NCF after electrochemical reduction. (e) Partial current densities of BNUS/NCF for HCOOH production at different densities. (f) Gibbs free energy of the rate-determining step for the polycrystalline Bi toward various reduction reactions. Reproduced with permission from ref 35. Copyright 2020 Wiley-VCH.

hydroxide nanosheet arrays on SS (SSNNi) were prepared via the simple hydrothermal treatment. This electrode exhibits low OER overpotential and long-term durability, and the Tafel slope of SSNNi is 36 mV dec^{-1} even smaller than that of RuO_2 (62 mV dec^{-1}) and Ir/C (120 mV dec^{-1}).[29] Furthermore, inspired by the rust and corrosion of iron in our daily life, we propose a strategy to synthesize a desirable SS OER electrode through in situ activating ubiquitous rust SS with the combination of corrosion treatment in the presence of ammonium solution and electrochemical oxidation−reduction cycle (EORC) (Figure 2g).[30] And higher content of Fe/(Ni)OOH is harvested by the EORC-activated rusty SS compared with the single-processing approach of EORC-activated or hydrothermal treatment and pure SS electrode. As a result, the overpotential of EORC-activated rusty SS reaches 0.26 V, which is even lower than commercial RuO_2 (0.32 V). Impressively, the slight decrease in OER activity upon long-term operation can be recovered through another EORC process (Figure 2h). Importantly, other types of SS can also be activated as effective OER electrodes by this hydrothermal corrosion and EORC (Figure 2i). This effective strategy for constructing robust OER electrode opens new avenues for the recycling of rusty SS, which is of great importance for industrial applications.

3. STORAGE OF HYDROGEN: SYNTHESIS OF FORMIC ACID AND AMMONIA

With the increasing CO_2 emission, the climate problem is becoming more serious, so the conversion of CO_2 to value-added chemicals has attracted great research interest. Electrochemical CO_2 reduction into HCOOH is one available choice due to the fast two-electron transfer reaction rate compared to other more complex reductions and the important value of HCOOH as hydrogen storage liquid. However, the activity and selectivity of the current electrocatalyst is far behind the application. We found that adjusting the formation and desorption of key intermediates of HCOO*/COOH*, CO_2^* is a crucial principle for the optimization of catalysts.

Except for HCOOH, NH_3, containing 17.6 wt % hydrogen storage, which is synthesized through NRR or NO_3RR, demonstrates more tremendous potential in the field of hydrogen storage. Similarly, the electrocatalysts for NH_3 synthesis also encounter unsatisfactory performance due to the inertness and the low solubility of N_2 and slow reaction kinetics. Additionally, the synthesis of HCOOH and NH_3 both face poor selectivity of low FE due to the competing HER. Therefore, highly efficient catalysts are needed to accelerate the reaction kinetics and suppress the competing HER toward high activity and selectivity.

3.1. Catalysts for HCOOH Synthesis

In terms of the efficient electrocatalysts for the electrochemical CO_2 reduction for the formate or formic synthesis, large FE for the selectivity, high partial current density of formate, high energy conversion efficiency, and stability are required.[5] Thanks to the advance in the in situ characterizations, it was verified that many electrocatalysts will undergo a dynamic reconstruction during the catalytic reaction process. The reconstruction strategy was subsequently developed for the electrocatalyst fabrication by controlling the structure and composition. Huang et al. proposed that the selectivity of CO_2RR can be tailored by changing the synthetic temperature of the copper (Cu) catalyst, which altered the exposed crystal face.[31] In addition, the precursor is important to affect the composition and architecture of the electrocatalyst after electrochemical reconstruction of Cu-based metal−organic frameworks (MOFs). Here, we constructed three types of Cu tetrazolate based MOFs for electrochemical CO_2RR.[32] Thereinto, Cu-5H (the ligand was 5H-tetrazole) exhibited the best

https://doi.org/10.1021/accountsmr.3c00197
Acc. Mater. Res. 2024, 5, 160−172

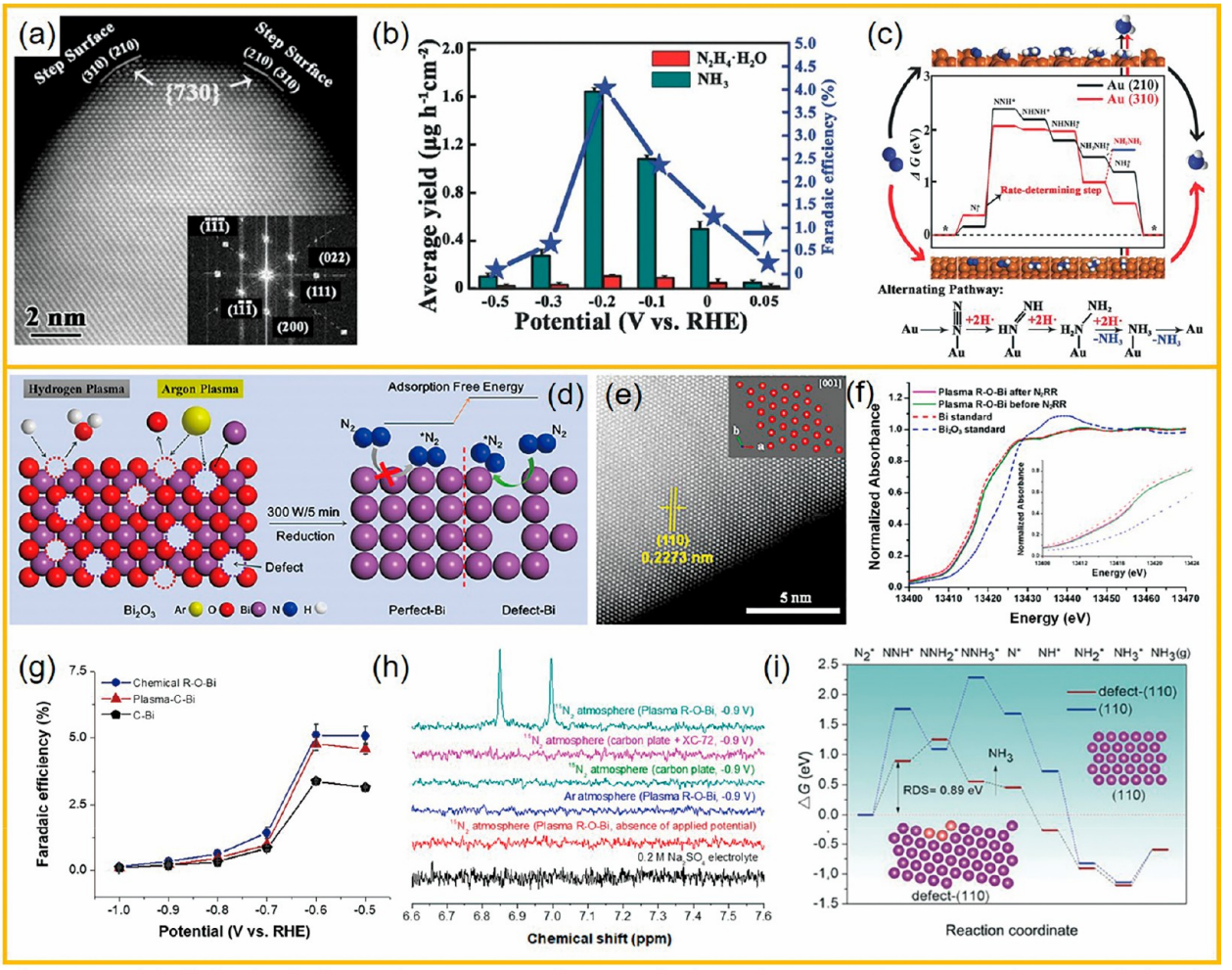

Figure 4. (a) Spherical aberration-corrected transmission electron microscope image of the Au NR. (b) Yield rate of NH_3, $N_2H_4{\cdot}H_2O$, and FEs at each given potential. (c) Free energy diagram and alternating pathway for NRR. Reproduced with permission from ref 38. Copyright 2016 Wiley-VCH. (d) Illustration of the preparation of Plasma R−O-Bi. (e) HRTEM image of Plasma R−O-Bi catalysts. (f) Bi L_{III}-edge XANES spectra of different catalysts. (g). FEs of different catalysts. (h) ^1H nuclear magnetic resonance (NMR) spectra of the electrolyte under different conditions. (i) Free energy diagram of ideal Bi (110) and defective Bi (110). Reproduced with permission from ref 40. Copyright 2019 Wiley-VCH.

CO_2RR performance with HCOOH FE of 91% at −0.8 V vs RHE which can be explained by the larger surface area and higher content metallic Cu species. Besides, bismuth (Bi) based catalysts such as BiOBr, Bi_2O_3, etc., would be transformed into metallic Bi during electrochemical CO_2 reduction, which was the active component.[33] Ultrathin BiOBr nanosheets (Bi-NSS) with large surface area and low coordination steps were developed to facilitate the CO_2RR process, which exhibited an enhanced current density of 15.1 mA cm^{-2} with the highest FE of 98.4% under CO_2 atmosphere compared with the nanospheres (Bi-SS) and nanoflowers (Bi-FS) counterparts (Figure 3a, b).[34] Owing to the high FEs of Bi-NSS, the highest energy efficiency of ∼60% at −1.1 V vs RHE is also gained in comparison with its counterparts (Figure 3c). Furthermore, through constructing 3D integrated electrode architecture for exposing more active sites and facilitating mass transfer, the in situ generated Bi based electrocatalytic electrode derived from the Bi_2O_3 ultrathin nanosheets/N-doped carbon foam (BNUS/NCF) demonstrated further improved catalytic activity and stability.[35] Meanwhile, the ultrathin Bi nanosheets contain numerous low-coordinated steps and edges, which would expose more interior atoms during reconstruction (Figure 3d). As a result, this catalyst displayed an enhanced HCOOH partial current density of 24.4 mA cm^{-2} at −1.1 V vs RHE (Figure 3e) and exhibited a maximal energy efficiency of 60.3% at −1.0 V vs RHE. DFT calculation demonstrates that Bi (110) possesses lower energy barrier of forming both HCOO* and COOH* during HCOOH synthesis in comparison with Bi (104) and Bi (012) (Figure 3f).

3.2. Catalysts for NH_3 Synthesis

Metal catalysts with unsaturated coordination states have witnessed a great progress in various catalysis. For example, theoretical reports have demonstrated that the stepped facets of the noble metal are the favorable active sites.[36,37] In 2017, we proposed and demonstrated that high-index facets of Au nanorods (NRs) (Figure 4a), which were prepared through a seeded growth method, can realize NH_3 synthesis from electrocatalytic N_2 reduction reaction in aqueous electrolyte under ambient conditions, along with the average NH_3 yield rate of 1.648 $\mu g\ h^{-1}\ cm^{-2}$ and 0.102 $\mu g\ h^{-1}\ cm^{-2}$ of $N_2H_4{\cdot}H_2O$ (Figure 4b).[38] The Au NRs are enclosed by (210) and (310) subfacets and contain unsaturated coordination, which exhibited a lower activation energy for NRR of 13.704 kJ mol^{-1}, than that of Haber−Bosch process (335 kJ mol^{-1})

https://doi.org/10.1021/accountsmr.3c00197
Acc. Mater. Res. 2024, 5, 160−172

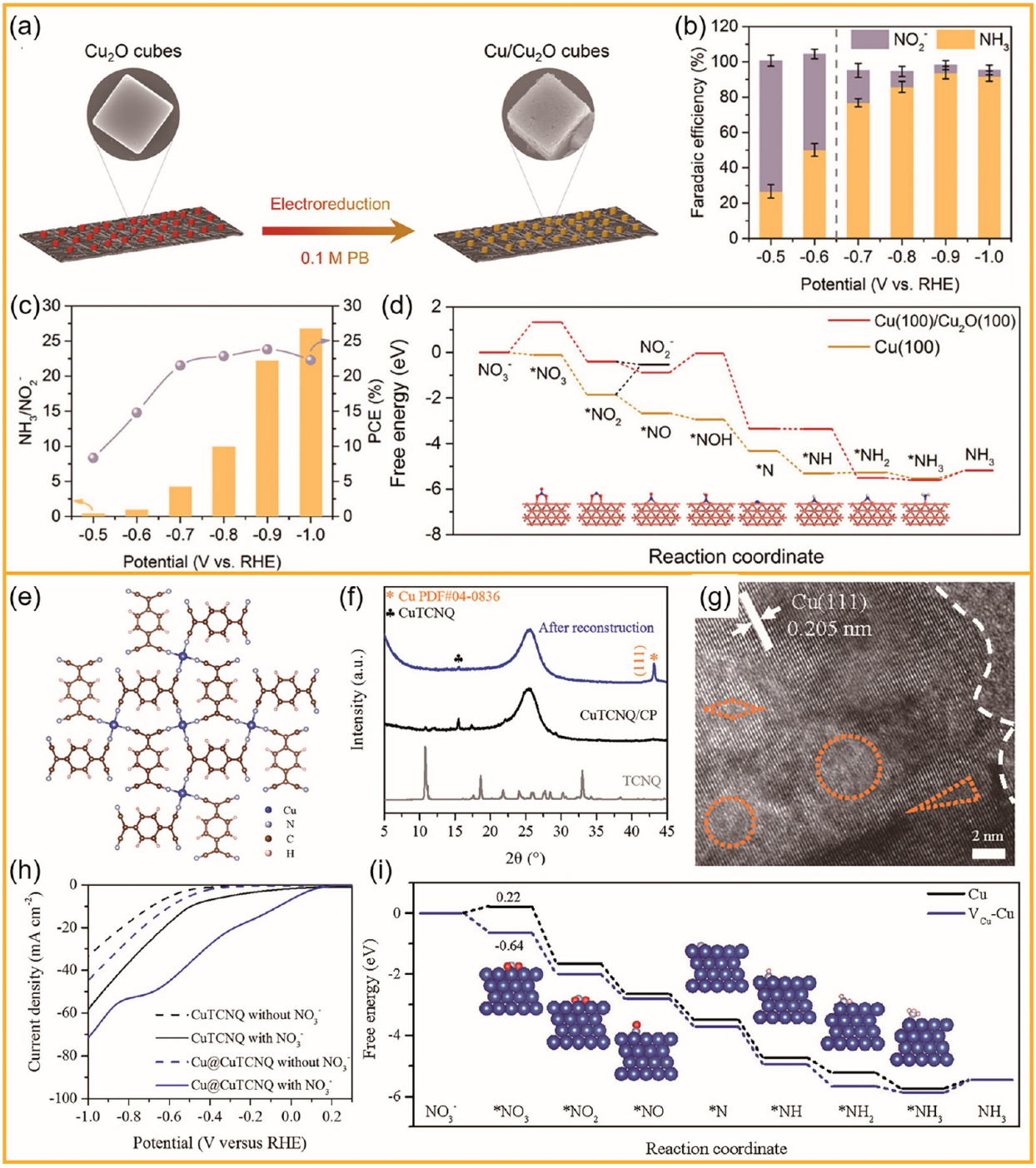

Figure 5. (a) Illustration of the construction of model Cu/Cu_2O catalysts. (b) FEs of NH_3 and NO_2^- under 0.1 M phosphate buffer (PB) and 0.1 M KNO_3 electrolyte over Cu/Cu_2O catalysts. (c) The ratio of FEs for NH_3 and NO_2^- and the cathodic power conversion efficiency. (d) Gibbs free energy of different samples for NH_3 and NO_2^- synthesis. Reproduced with permission from ref 43. Copyright 2023 American Chemical Society. (e) Chemical structure of CuTCNQ. (f) XRD pattern of Cu@CuTCNQ obtained by electrochemical reconstruction. (g) HRTEM image of Cu@CuTCNQ and the orange dashed boxes are Cu vacancy defects. (h) LSV curves of Cu@CuTCNQ and CuTCNQ with or without NO_3^-. (i) Gibbs free energy diagram of eNO_3RR over Cu and V_{Cu}−Cu. Reproduced with permission from ref 44. Copyright 2023 Elsevier.

without catalysts. Combined theoretical calculations and experimental results, a possible NRR process is proposed (Figure 4c): (I) N_2 first adsorbed on the Au facets due to the unsaturated coordination; (II) the activated H combined with N_2 to form stable N−H to break the stable N≡N bond; (III) the NH_3 was generated by adding H atoms one-by-one.

Defect engineering is another effective strategy to optimize the coordination state of the catalysts, which is relevant to the adsorption energy of the reactants and intermediates on active sites.[39] In our group, defect-rich bismuth nanoplate (Plasma R−O−Bi) was constructed by low temperature plasma treatment with Bi_2O_3 and applied as NRR electrocatalyst (Figure 4d, e).[40]

We found that the numerous lattice-isolated Bi vacancy defect shows lower Bi−Bi bond coordination number than the ideal Bi (Figure 4f) upon XANES analysis. Compared with the

https://doi.org/10.1021/accountsmr.3c00197
Acc. Mater. Res. 2024, 5, 160−172

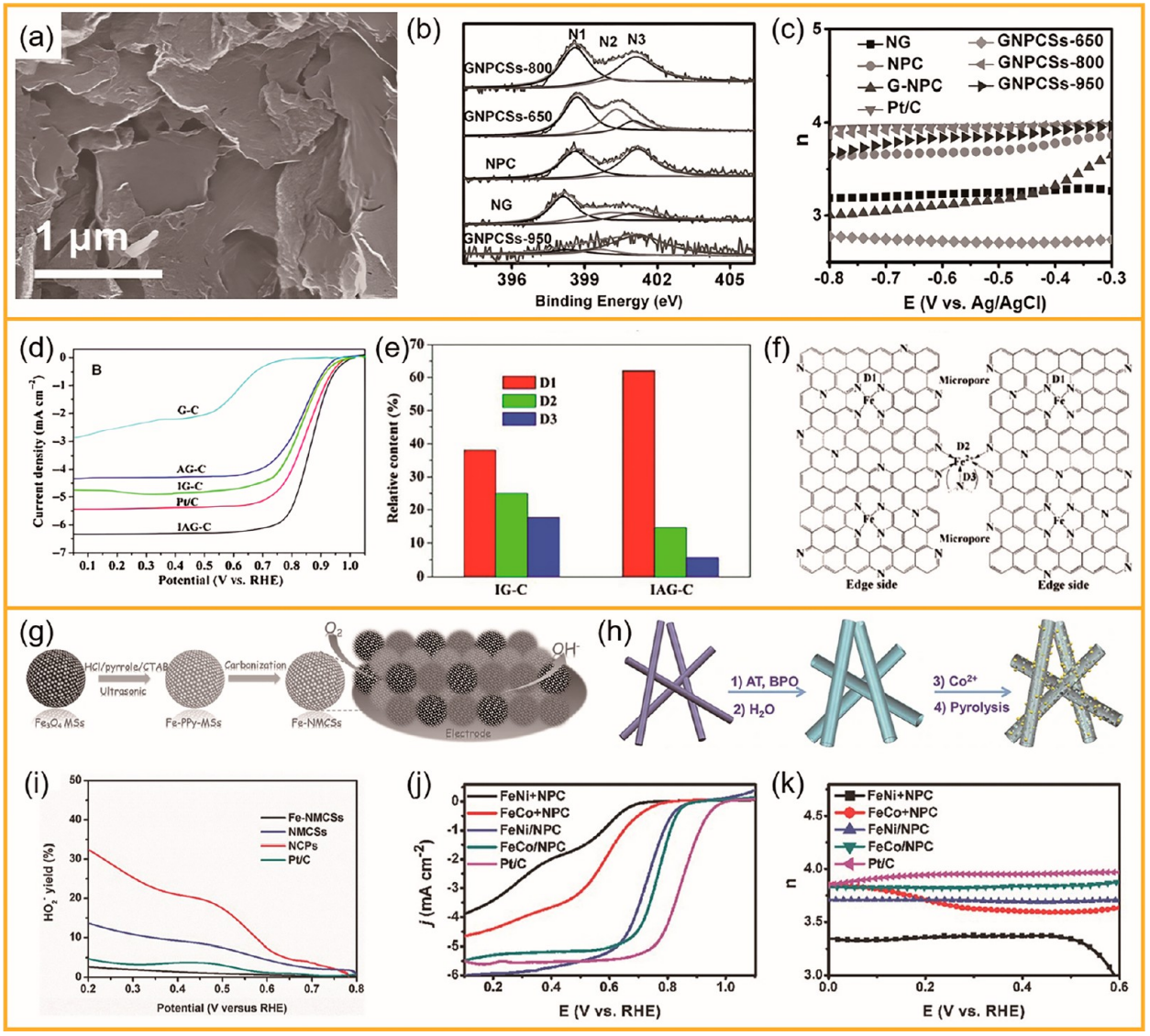

Figure 6. (a) SEM image of GNPCSs-800. (b) High-resolution N 1s spectra of different catalysts. (c) Electron transfer numbers of different catalysts based on RRDE data. Reproduced with permission from ref 47. Copyright 2014 Wiley-VCH. (d) LSV curves of different catalysts under O_2-saturated 0.1 M KOH electrolyte. (e) Relative content of D1, D2, and D3 in IG-C and IGA-C. (f) Proposed structure model of IAG-C. Adapted with permission under a Creative Commons (open access) license from ref 50. Copyright 2015 Zhongli Wang et al. (g) Scheme of in situ construction of Fe-NMCSs. Reproduced with permission from ref 54. Copyright 2016 Wiley-VCH. (h) Scheme of in situ construction of Co_9S_8/NSPC. Adapted with permission under a Creative Commons (open access) license from ref 55. Copyright 2016 Haixia Zhong et al. (i) LSV curves of ORR under O_2-saturated 0.1 M KOH. Reproduced with permission from ref 54. Copyright 2016 Wiley-VCH. (j) ORR polarization curves. (k) Electron transfer numbers of different catalysts. Reproduced with permission from ref 56. Copyright 2017 Wiley-VCH.

chemical reduction Bi catalyst (Chemical R−O−Bi), Plasma R−O−Bi exhibited a high catalytic performance for electrochemical N_2 reduction reaction to ammonia with $^{15}NH_3$ yield rate of 5.453 μg mg_{Bi}^{-1} h^{-1} and 11.68% FE under ambient conditions (Figure 4g, h). Such defective Bi is more favorable for the adsorption and activation of N_2 to form key intermediate of N_2H^*, and the activation energy of the defective Bi facet is lower than that of ideal Bi, indicating more favorable reaction kinetics (Figure 4i).

Compared with NRR, NO_3RR possesses faster reaction kinetics due to the lower dissociation energy of N═O bond whereas the undesirable side products of NO_2^- and H_2 species will decrease the FE of NH_3 synthesis. Cu based catalysts have been widely reported to exhibit great potential for NO_3RR due to its suitable adsorption of intermediates and suppression of HER.[41,42] However, the real catalytic structure and its correlation with the activity and selectivity remain unclear due to the easy oxidation of Cu and probing limitations. Consequently, a Cu/Cu_2O model catalyst was fabricated through electrochemical prereduction of Cu_2O particles to investigate the effect of the chemical state on the product selectivity (Figure 5a).[43] In situ Raman and ex situ XRD disclosed the transformation of metallic Cu from Cu/Cu_2O under the potential negative than −0.6 V vs RHE. It was proposed that metallic Cu site with low energy barrier is in favor of generating NH_3, while Cu/Cu_2O interface tends to the formation of NO_2^- (Figure 5b−d). Finally, this oxide-derived Cu^0 (OD-Cu-c) achieves a high NH_3 FE of 93.9% and NH_3 yield rate of 219.8 μmol h^{-1} cm^{-2} along with the highest power conversion efficiency of 23.8% at −0.9 V vs RHE. Guided by

https://doi.org/10.1021/accountsmr.3c00197
Acc. Mater. Res. 2024, 5, 160−172

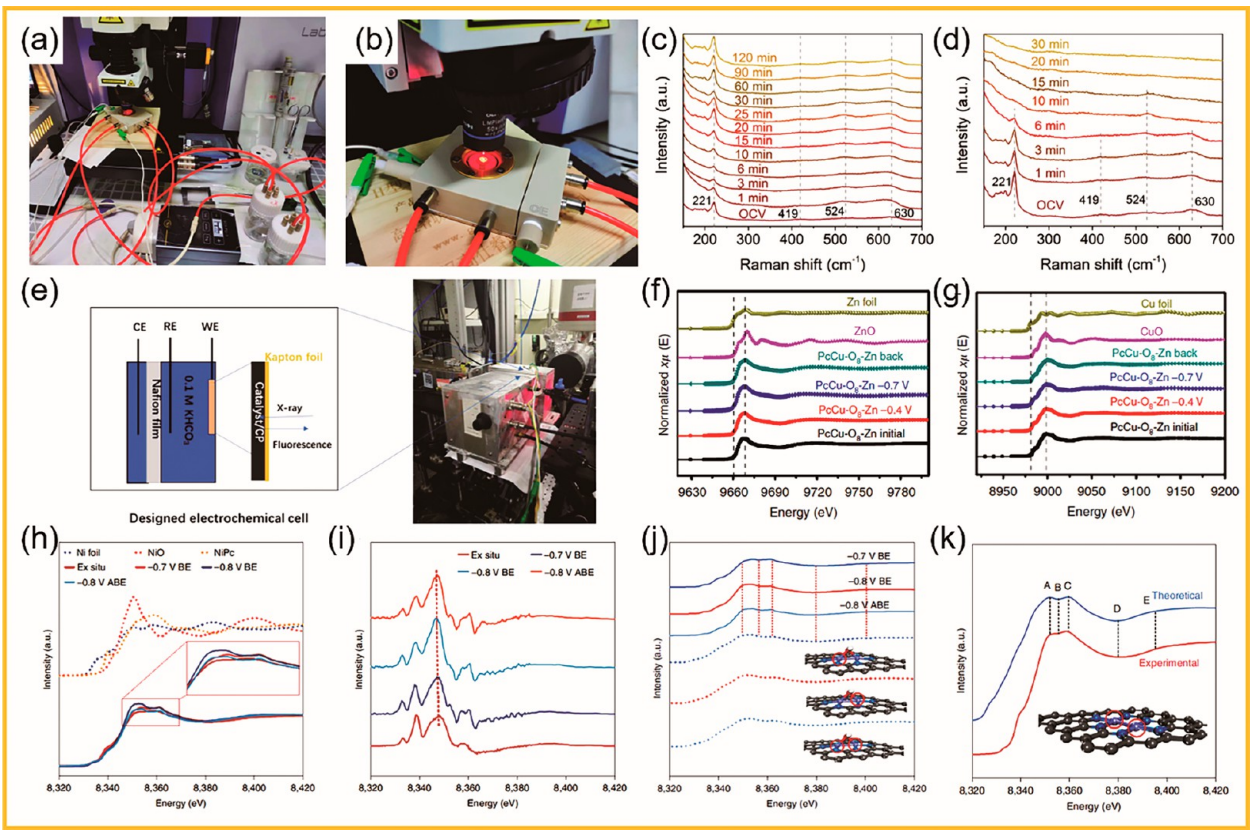

Figure 7. (a, b) Photograph of in situ Raman instrument for NO_3RR. (c, d) Raman spectra of OD-Cu-c under NO_3RR at −0.6 V and −0.9 V vs RHE. Reproduced with permission from ref 43. Copyright 2023 American Chemical Society. (e) Photograph of *in situ* XAS setup for CO_2RR. (f) Operando Zn K-edge XANES spectra. (g) In situ Cu K-edge XANES spectra. Adapted with permission under a Creative Commons (open access) license from ref 58. Copyright 2020 Haixia Zhong et al. (h) In situ Ni K-edge Ni_2NC at different potentials; BE and ABE represent bulk electrolysis and after bulk electrolysis, respectively. (i) The first derivative of XANES. (j) In situ XANES spectra (solid lines) and corresponding theoretical spectra (dotted lines) at different applied potentials. (k) Ex situ XANES spectrum and theoretical spectrum for Ni_2NC. Reproduced with permission from ref 60. Copyright 2022 Nature Spring.

this conclusion, we also fabricated the copper and copper-tetracyanoquinodimethane composite catalyst (Cu@CuTCNQ) with abundant Cu vacancy by the electrochemical reconstruction of CuTCNQ MOF toward enhancing NO_3RR (Figure 5e–h).[44] The results show that Cu@CuTCNQ enhances the adsorption of NO_3^-, decreases the reaction barrier, and inhibits the HER, thereby improving the NO_3RR performance (Figure 5i).

4. UTILIZATION OF HYDROGEN: FUEL CELL

Fuel cell, exhibiting high energy density, high conversion efficiency, and nonpollution, is a promising pathway for H_2 energy utilization. While the oxygen reduction reaction (ORR) is generally considered as the bottleneck of fuel cells because of its sluggish kinetics. Usually, ORR proceeds within two pathways of two-electron ($O_2 + 2H^+ + 2e^- \rightarrow H_2O_2$) and four-electron ($O_2 + 4H^+ + 4e^- \rightarrow 2H_2O$) process. And four proton–electron ORR process to form water is desirable for high-efficiency fuel cells.[10] Pt and its alloys were regarded as the best ORR catalysts, whereas high cost and reserve scarcity hindered their large-scale application.[45] Therefore, highly efficient and selective low-cost catalysts need to be developed to promote ORR.

Carbon-based materials have shown great potential owing to their large surface area and modifiable surface. The N doping into carbon materials can induce charge redistribution of C sites to improve the ORR activity, wherein the C sites close to the resulting pyridinic-N and graphitic-N are commonly recognized as the active species.[46] In terms of the important role of C and N components and the 2D catalytic structure in promoting the catalytic performance, we developed sandwich-like N doped porous carbon on graphene sheets as the ORR electrocatalyst (Figure 6a, b).[47] The combination of zeolitic imidazolate framework (ZIF-8) and graphene oxide (GO) contributes to achieving porous architecture, considerable nitrogen content, and good conductivity. Besides, the change of carbonization temperature tailors the content and type of doped N, in which the sample obtained at 800 °C (GNPCSs-800) realized the optimum activity with an electron transfer number of 3.98, close to the value of Pt/C (4.0) (Figure 6c).

NC exhibits great advantages for ORR due to the large surface area, high mass transportation, and efficient utilization of active catalytic sites. Moreover, the anchoring of transition metals on NC to form M–N (e.g., Fe–N, Co–N) sites can further improve the ORR activity, wherein the coordination configuration of metal is important.[48,49] Unfortunately, the agglomeration and inhomogeneity of metal dispersion is still challenging. To alleviate this issue, a novel strategy based on the sol–gel chemistry of gelatin biomolecule and iron nitrate was developed.[50] And the obtained Fe–N–C catalysts exhibit outstanding performance in both alkaline and acidic electrolytes with nearly four-electron transfer (Figure 6d). By means

https://doi.org/10.1021/accountsmr.3c00197
Acc. Mater. Res. 2024, 5, 160–172

of ^{57}Fe Mössbauer spectroscopy, the high activity might be related to the high content of D1+D3 sites (Figure 6e, f). After that, further research demonstrated that D3 site showed higher intrinsically activity but with less stability, while D1 site exhibited better stability along with inferior activity.[51,52] Therefore, catalysts with high density of D1 site would be more attractive. Additionally, we implemented homogeneous Fe dispersion on N-containing polymer through a novel iron-chelated urea-formaldehyde resin (UFR) hydrogel method.[53] This electrocatalyst showed positive onset potential of 1.02 V vs RHE and an electron transfer number of ∼4.

Furthermore, in situ coupling of metal and NC materials approach is developed to guarantee high electron conductivity, avoid metal detachment from the substrate, and provide more active sites for ORR (Figure 6g, h).[54,55] For example, Fe−N-doped mesoporous carbon microspheres (Fe-NMCSs) that are constructed via in situ replication and polymerization strategy,[54] provides large surface and favorable mass transfer. The high content of pyridinic-N, quaternary-N, and the existence of iron ions synergistically promote the intrinsic ORR activity along with low H_2O_2 selectivity (Figure 6i). Besides, transition metals other than Fe, such as Co, Ni, etc., also displayed great potential as ORR electrocatalysts.[55−57] For instance, in situ coupling FeNi and FeCo particles with nitrogen-doped porous carbon (FeNi/NPC, FeCo/NPC) expressed the electron transfer number of 3.83 and 3.8 with HO_2^- yield less than 10% toward ORR.[56] Surprisingly, these catalysts can also realize highly efficient water splitting of OER and HER. Furthermore, in situ anchoring Co_9S_8 on N and S codoped porous carbon tube (Co_9S_8/NSPC) largely promoted the ORR performance with more positive half-wave potential and high durability with electron transfer number of 3.94 (Figure 6j, k).[55]

5. ADVANCES IN CATALYTIC MECHANISM STUDIES

Advances in characterization techniques and theoretical calculations offered more opportunities for insightful studies on the real catalytic sites and catalytic mechanisms, which is of great importance to guide the rational catalyst design. For example, in situ/operando characterizations (e.g., in situ XAS, in situ Raman/FT-IR) were applied to obtain more information about the chemical state and coordination structure of catalysts, as well as the adsorption of intermediates during the catalytic reaction process. Recently, we demonstrated that the selective NO_3RR for NH_3 synthesis is related to the chemical state of Cu-based catalysts using the in situ Raman analysis and DFT calculations. By combining with the in situ characterizations and theoretical calculations (Figure 7a−d), the catalytic pathway was also identified.[43] In situ Raman and in situ attenuated total reflectance-Fourier transform infrared spectroscopy (ATR-FTIR) demonstrated that the true catalytic site is metallic phase Cu^0 for the promotion of NH_3 selectivity from NO_3^-. Note that, following this result, we constructed the defect-rich Cu@CuTCNQ and achieved high catalytic performance for NO_3RR to NH_3 with a high FE of 96.4% and yield rate of 144.8 μmol h^{-1} cm^{-2} at −0.6 V vs RHE in alkaline electrolyte.[44]

Besides, in situ XAS has been applied to explore the fine structure of catalytic materials during the electrochemical conversion process and provide key information for investigating the relationship between structure and catalytic performance. Zhong et al. verified the stable valence state of Zn (II) and Cu (II) by means of in situ XANES during the CO_2RR process over their PcCu-O_8−Zn/CNT catalyst (Figure 7e−g). Combined with in situ EXAFS, they claimed that the catalytic centers are stable ZnO_4 and CuN_4 sites without the formation of metals or metal clusters.[58] Similarly, during electrochemical NRR process, in situ XANES analysis displayed the compression of Fe−N coordination bond and demonstrated that this is due to the interaction between the adsorbed intermediates and Fe sites over FePc-pz catalysts, proposing that the real catalytic sites were Fe−N_4.[59] Except for the chemical state and coordination structure, the real microenvironment of the catalysts also influences the catalytic performance. In our Ni dual-atom catalyst (DACs) system,[60] through using the in situ XAS, we found that hydroxide ions will be spontaneously adsorbed on Ni dual-atom sites upon applying the potential, which is considerably different from the Ni_2NC powder samples (Figure 7h−j), and thus affect the microenvironment around the Ni active sites. Combined with theoretical calculations, it was concluded that the adsorption of hydroxyl (OH_{ad}) on Ni active sites during the CO_2RR process (Figure 7k) could result in the electron-rich microenvironment of Ni sites and reduce the energy barrier of the rate-determining step toward a fast reaction kinetics. Thus, experimental and theoretical results synergistically demonstrated that the rapid CO_2RR kinetics for Ni DACs derived from the contribution to the *COOH formation and *CO desorption.

6. CONCLUSIONS AND OUTLOOK

In conclusion, we outline our efforts in the development of efficient electrocatalysts by regulation of coordination and architecture structure and the studies on the mechanism of performance optimization to address the main challenges of hydrogen energy conversion. Although progress on the improvement of hydrogen energy conversion efficiency has been made through constructing effective electrocatalysts over these years, problems in exploring highly effective electrocatalysts still remain, and more effective technologies and a deeper fundamental understanding should be input into this field.

The enhancement mechanisms on catalytic process are still unclear, and the causes of the performance degradation are lack of in-depth analysis. Despite the progress on monitoring the change of the catalytic structure under the operating condition, the investigation on real catalytic environment is still insufficient due to the limitation of the characterization strategy. Especially, the solvent effect should be taken more into account, such as the coordination structure of water on the active sites, the ion effects of K^+, OH^- in electrolyte, etc., which will affect the microenvironment of the catalytic sites. On the other hand, the discrepancy between the well-designed system for the catalyst performance assessment and its real working conditions in the fuel cell and electrolytic tank should not be neglected. Importantly, more attentions on the in-depth analysis of the performance degradation under the operation of the device through the advanced in situ/ex-situ characterization techniques are needed, which is crucial for the commercial applications.

The synthetic technique on the highly active and economic catalysts needs to be promoted. Theoretical studies have predicted the highly active coordination structure for the electrocatalytic reaction. However, it is full of challenges, such as how to boot the rational design of the catalyst effectively, precisely control the construction of these designed catalyst,

https://doi.org/10.1021/accountsmr.3c00197
Acc. Mater. Res. 2024, 5, 160−172

and efficiently explore the synthesis approaches for the large-scale preparation of materials. In terms of these issues, the application of artificial intelligence (AI) and machine learning (ML) technologies would be one appealing choice to facilitate the development of low-cost catalysts. Besides, the simplification of synthesis process is also important for the commercial applications. In the future application of H_2 energy, three-dimensional porous integrated electrode, which have oriented porous architecture, large number of highly active sites and structural stability against the corrosion by the electrolyte and the applied potential, will exhibit potentially commercial applications possess due to the high activity, the faster electron/mass transfer capability, and better stability. Then a rational membrane electrode assembly (MEA) reactor with low loading of effective and low-cost catalyst and optimized architecture is highly needed for the high-efficiency H_2 application.

Meanwhile, the application of H_2 energy will inevitably depend on renewable energy such as solar and wind energy, thus the breakthroughs of sustainable energy technologies are also crucial for realizing zero carbon emission. The storage and transportation of H_2 still face great challenges, then the development of NH_3−H_2 pathway shows enormous potential on application prospects. Apart from the H_2 storage media, NH_3 is expected to be an as H_2 energy carrier if the synthetic system can be well developed because NH_3 can overcome the limitation of production, transportation, and storage of H_2. Therefore, the investigation of efficient catalysts, suitable technologies, and integrated systems for the production, transportation, and storage of H_2 and NH_3 is of great importance for the future H_2 economy.

AUTHOR INFORMATION

Corresponding Authors

Xin-bo Zhang − *State Key Laboratory of Rare Earth Resource Utilization, Changchun Institute of Applied Chemistry, Chinese Academy of Sciences, Changchun 130022, P. R. China; School of Applied Chemistry and Engineering, University of Science and Technology of China, Hefei 230026, P. R. China;* orcid.org/0000-0002-5806-159X; Email: xbzhang@ciac.ac.cn

Hai-xia Zhong − *State Key Laboratory of Rare Earth Resource Utilization, Changchun Institute of Applied Chemistry, Chinese Academy of Sciences, Changchun 130022, P. R. China; School of Applied Chemistry and Engineering, University of Science and Technology of China, Hefei 230026, P. R. China;* orcid.org/0000-0002-2839-0253; Email: hxzhong@ciac.ac.cn

Authors

Miao-miao Shi − *Key Laboratory of Automobile Materials, Ministry of Education and Department of Materials Science and Engineering, Jilin University, Changchun 130012, P. R. China*

Di Bao − *State Key Laboratory of Rare Earth Resource Utilization, Changchun Institute of Applied Chemistry, Chinese Academy of Sciences, Changchun 130022, P. R. China*

Jun-min Yan − *Key Laboratory of Automobile Materials, Ministry of Education and Department of Materials Science and Engineering, Jilin University, Changchun 130012, P. R. China;* orcid.org/0000-0001-8511-3810

Complete contact information is available at: https://pubs.acs.org/10.1021/accountsmr.3c00197

Notes

The authors declare no competing financial interest.

Biographies

Miao-miao Shi received her Ph.D degree at Jilin University and currently works here as a postdoctoral fellow. Her work focuses on the design and preparation of highly efficient catalytic materials toward the conversion clean energy, especially the synthesis of ammonia under mild conditions.

Di Bao is an associate researcher at State Key Laboratory of Rare Earth Resource Utilization, Changchun Institute of Applied Chemistry. He received Ph.D. degree from Harbin Engineering University. His research interests are ammonia−hydrogen conversion, high-temperature electrochemistry, and energy conversion devices.

Jun-min Yan is a professor at Key Laboratory of Automobile Materials, Ministry of Education and Department of Materials Science and Engineering, Jilin University. She received her Ph.D. degree at Changchun Institute of Applied Chemistry. Her research interests lie in development of new functional materials for (renewable) energy storage and conversion applications.

Hai-xia Zhong is a professor at State Key Laboratory of Rare Earth Resource Utilization, Changchun Institute of Applied Chemistry, Chinese Academy of Sciences. She received her Ph.D. degree at University of Chinese Academy of Sciences in 2017. Her research interests mainly focus on catalytic materials for efficient electrochemical energy storage and conversion, such as electrocatalysis reduction/oxidation of water, nitrogen, oxygen, and carbon dioxide, as well as the development of high-temperature solid oxide electrolysis cell and fuel cell.

Xin-bo Zhang joined CIAC as a professor of the "Hundred Talents Program" of the Chinese Academy of Sciences in 2010. He received his Ph.D. degree at Changchun Institute of Applied Chemistry. During 2005−2010, he worked as a JSPS and NEDO fellow at the National Institute of Advanced Industrial Science and Technology (Kansai center), Japan. His interests mainly focus on functional inorganic materials for energy storage and conversion with fuel cells and novel batteries, especially lithium−air batteries.

ACKNOWLEDGMENTS

This work was supported by National Key R&D Program of China (2020YFE0204500), the National Natural Science Foundation of China (52273277 and 52072362), Jilin Province Science and Technology Development Plan Funding Project (20220201112GX), and Youth Innovation Promotion Association CAS (2021223). H.X.Z. acknowledges funding from National Natural Science Foundation of China Outstanding Youth Science Foundation of China (Overseas).

REFERENCES

(1) Abnisa, F.; Arami-Niya, A.; Daud, W. M. a. W.; Sahu, J. N. Characterization of Bio-oil and Bio-Char from Pyrolysis of Palm Oil Wastes. *BioEnergy Res.* **2013**, *6* (2), 830−840.

(2) Zhang, X. J.; Liu, H.; Yang, G. Y.; Wang, Y. P.; Yao, H. Comprehensive Insights into the Application Strategy of Kitchen Waste Derived Hydrochar: Random Forest-Based Modelling. *Chem. Eng. J.* **2023**, *469*, 143840.

(3) Zhang, X. Y.; Schwarze, M.; Schomäcker, R.; Van De Krol, R.; Abdi, F. F. Life Cycle Net Energy Assessment of Sustainable H_2

Production and Hydrogenation of Chemicals in a Coupled Photoelectrochemical Device. *Nat. Commun.* **2023**, *14* (1), 991.
(4) Jiao, Y. Q.; Yan, H. J.; Tian, C. G.; Fu, H. G. Structure Engineering and Electronic Modulation of Transition Metal Interstitial Compounds for Electrocatalytic Water Splitting. *Acc. Mater. Res.* **2023**, *4* (1), 42−56.
(5) Liu, K. H.; Zhong, H. X.; Li, S. J.; Duan, Y. X.; Shi, M. M.; Zhang, X. B.; Yan, J. M.; Jiang, Q. Advanced Catalysts for Sustainable Hydrogen Generation and Storage Via Hydrogen Evolution and Carbon Dioxide/Nitrogen Reduction Reactions. *Prog. Mater. Sci.* **2018**, *92*, 64−111.
(6) Lin, L.; Ni, Y. X.; Shang, L.; Sun, H. X.; Zhang, Q.; Zhang, W.; Yan, Z. H.; Zhao, Q.; Chen, J. Atomic-Level Modulation-Induced Electron Redistribution in Co Coordination Polymers Elucidates the Oxygen Reduction Mechanism. *ACS Catal.* **2022**, *12* (13), 7531−7540.
(7) Mehmood, A.; Gong, M.; Jaouen, F.; Roy, A.; Zitolo, A.; Khan, A.; Sougrati, M.-T.; Primbs, M.; Bonastre, A. M.; Fongalland, D.; Drazic, G.; Strasser, P.; Kucernak, A. High Loading of Single Atomic Iron Sites in Fe-NC Oxygen Reduction Catalysts for Proton Exchange Membrane Fuel Cells. *Nat. Catal.* **2022**, *5* (4), 311−323.
(8) Zeng, Y.; Zhao, M. T.; Huang, Z. H.; Zhu, W. J.; Zheng, J. X.; Jiang, Q.; Wang, Z. W.; Liang, H. F. Surface Reconstruction of Water Splitting Electrocatalysts. *Adv. Energy Mater.* **2022**, *12* (33), 2201713.
(9) You, B.; Tang, M. T.; Tsai, C.; Abild-Pedersen, F.; Zheng, X. L.; Li, H. Enhancing Electrocatalytic Water Splitting by Strain Engineering. *Adv. Mater.* **2019**, *31* (17), 1807001.
(10) Seh, Z. W.; Kibsgaard, J.; Dickens, C. F.; Chorkendorff, I.; Norskov, J. K.; Jaramillo, T. F. Combining Theory and Experiment in Electrocatalysis: Insights into Materials Design. *Science* **2017**, *355* (6321), No. eaad4998.
(11) Lu, M.; Zheng, Y.; Hu, Y.; Huang, B. L.; Ji, D. G.; Sun, M. Z.; Li, J. Y.; Peng, Y.; Si, R.; Xi, P. X.; Yan, C. H. Artificially Steering Electrocatalytic Oxygen Evolution Reaction Mechanism by Regulating Oxygen Defect Contents in Perovskites. *Sci. Adv.* **2022**, *8* (30), No. eabq3563.
(12) Li, Y. J.; Sun, Y. J.; Qin, Y. N.; Zhang, W. Y.; Wang, L.; Luo, M. C.; Yang, H.; Guo, S. J. Recent Advances on Water-Splitting Electrocatalysis Mediated by Noble-Metal-Based Nanostructured Materials. *Adv. Energy Mater.* **2020**, *10* (11), 1903120.
(13) Zagalskaya, A.; Alexandrov, V. Role of Defects in the Interplay between Adsorbate Evolving and Lattice Oxygen Mechanisms of the Oxygen Evolution Reaction in RuO_2 and IrO_2. *ACS Catal.* **2020**, *10* (6), 3650−3657.
(14) Ping, Y.; Nielsen, R. J.; Goddard, W. A. The Reaction Mechanism with Free Energy Barriers at Constant Potentials for the Oxygen Evolution Reaction at the IrO_2 (110) Surface. *J. Am. Chem. Soc.* **2017**, *139* (1), 149−155.
(15) Mccrory, C. C. L.; Jung, S.; Ferrer, I. M.; Chatman, S. M.; Peters, J. C.; Jaramillo, T. F. Benchmarking Hydrogen Evolving Reaction and Oxygen Evolving Reaction Electrocatalysts for Solar Water Splitting Devices. *J. Am. Chem. Soc.* **2015**, *137* (13), 4347−4357.
(16) Zheng, Y.; Jiao, Y.; Zhu, Y. H.; Li, L. H.; Han, Y.; Chen, Y.; Du, A. J.; Jaroniec, M.; Qiao, S. Z. Hydrogen Evolution by a Metal-Free Electrocatalyst. *Nat. Commun.* **2014**, *5* (1), 3783.
(17) Zhong, H. X.; Zhang, Q.; Wang, J.; Zhang, X. B.; Wei, X. L.; Wu, Z. J.; Li, K.; Meng, F. L.; Bao, D.; Yan, J. M. Engineering Ultrathin C_3N_4 Quantum Dots on Graphene as a Metal-Free Water Reduction Electrocatalyst. *ACS Catal.* **2018**, *8* (5), 3965−3970.
(18) Mei, B. B.; Liu, C.; Sun, F. F.; Lu, S. Y.; Du, X. L.; Li, X. P.; Song, F.; Xu, W. L.; Jiang, Z. Unraveling the Potential-Dependent Volcanic Selectivity Changes of an Atomically Dispersed Ni Catalyst During CO_2 Reduction. *ACS Catal.* **2022**, *12* (14), 8676−8686.
(19) Xue, Y. R.; Huang, B. L.; Yi, Y. P.; Guo, Y.; Zuo, Z. C.; Li, Y. J.; Jia, Z. Y.; Liu, H. B.; Li, Y. L. Anchoring Zero Valence Single Atoms of Nickel and Iron on Graphdiyne for Hydrogen Evolution. *Nat. Commun.* **2018**, *9* (1), 1460.
(20) Tabassum, H.; Zou, R. Q.; Mahmood, A.; Liang, Z. B.; Guo, S. J. A Catalyst-Free Synthesis of B, N Co-Doped Graphene Nanostructures with Tunable Dimensions as Highly Efficient Metal Free Dual Electrocatalysts. *J. Mater. Chem. A* **2016**, *4* (42), 16469−16475.
(21) Sa, Y. J.; Park, S. O.; Jung, G. Y.; Shin, T. J.; Jeong, H. Y.; Kwak, S. K.; Joo, S. H. Heterogeneous Co-N/C Electrocatalysts with Controlled Cobalt Site Densities for the Hydrogen Evolution Reaction: Structure-Activity Correlations and Kinetic Insights. *ACS Catal.* **2019**, *9* (1), 83−97.
(22) Wang, Z. L.; Hao, X. F.; Jiang, Z.; Sun, X. P.; Xu, D.; Wang, J.; Zhong, H. X.; Meng, F. L.; Zhang, X. B. C and N Hybrid Coordination Derived Co-C-N Complex as a Highly Efficient Electrocatalyst for Hydrogen Evolution Reaction. *J. Am. Chem. Soc.* **2015**, *137* (48), 15070−15073.
(23) Wang, J.; Zhong, H. X.; Wang, Z. L.; Meng, F. L.; Zhang, X. B. Integrated Three-Dimensional Carbon Paper/Carbon Tubes/Cobalt-Sulfide Sheets as an Efficient Electrode for Overall Water Splitting. *ACS Nano* **2016**, *10* (2), 2342−2348.
(24) Li, J.; Zhu, Y. Y.; Chen, W.; Lu, Z. Y.; Xu, J. W.; Pei, A.; Peng, Y. C.; Zheng, X. L.; Zhang, Z. W.; Chu, S.; Cui, Y. Breathing-Mimicking Electrocatalysis for Oxygen Evolution and Reduction. *Joule* **2019**, *3* (2), 557−569.
(25) Wang, J.; Li, K.; Zhong, H. X.; Xu, D.; Wang, Z. L.; Jiang, Z.; Wu, Z. J.; Zhang, X. B. Synergistic Effect between Metal-Nitrogen-Carbon Sheets and NiO Nanoparticles for Enhanced Electrochemical Water-Oxidation Performance. *Angew. Chem., Int. Ed.* **2015**, *54* (36), 10530−10534.
(26) Yuan, C. Z.; Li, J. Y.; Hou, L. R.; Zhang, X. G.; Shen, L. F.; Lou, X. W. Ultrathin Mesoporous $NiCo_2O_4$ Nanosheets Supported on Ni Foam as Advanced Electrodes for Supercapacitors. *Adv. Funct. Mater.* **2012**, *22* (21), 4592−4597.
(27) Wang, J.; Zhong, H. X.; Qin, Y. L.; Zhang, X. B. An Efficient Three-Dimensional Oxygen Evolution Electrode. *Angew. Chem., Int. Ed.* **2013**, *52* (20), 5248−5253.
(28) Subbaraman, R.; Tripkovic, D.; Chang, K.-C.; Strmcnik, D.; Paulikas, A. P.; Hirunsit, P.; Chan, M.; Greeley, J.; Stamenkovic, V.; Markovic, N. M. Trends in Activity for the Water Electrolyser Reactions on 3d M(Ni,Co,Fe,Mn) Hydr(oxy)oxide Catalysts. *Nat. Mater.* **2012**, *11* (6), 550−557.
(29) Zhang, Q.; Zhong, H. X.; Meng, F. L.; Bao, D.; Zhang, X. B.; Wei, X. L. Three-Dimensional Interconnected $Ni(Fe)O_xH_y$ Nanosheets on Stainless Steel Mesh as a Robust Integrated Oxygen Evolution Electrode. *Nano Res.* **2018**, *11* (3), 1294−1300.
(30) Zhong, H. X.; Wang, J.; Meng, F. L.; Zhang, X. B. In Situ Activating Ubiquitous Rust Towards Low-Cost, Efficient, Free-Standing, and Recoverable Oxygen Evolution Electrodes. *Angew. Chem., Int. Ed.* **2016**, *55* (34), 9937−9941.
(31) Min, S.; Yang, X.; Lu, A. Y.; Tseng, C. C.; Hedhili, M. N.; Li, L. J.; Huang, K. W. Low Overpotential and High Current CO_2 Reduction with Surface Reconstructed Cu Foam Electrodes. *Nano Energy* **2016**, *27*, 121−129.
(32) Zhong, H. X.; Liu, K. H.; Zhang, Q.; Meng, F. L.; Bao, D.; Zhang, X. B. Copper Tetrazolate Based Metal-Organic Frameworks as Highly Efficient Catalysts for Artificially Chemical and Electrochemical CO_2 Conversion. *Nano Select* **2020**, *1* (3), 311−319.
(33) Gong, Q. F.; Ding, P.; Xu, M. Q.; Zhu, X. R.; Wang, M. Y.; Deng, J.; Ma, Q.; Han, N.; Zhu, Y.; Lu, J.; Feng, Z. X.; Li, Y. F.; Zhou, W.; Li, Y. G. Structural Defects on Converted Bismuth Oxide Nanotubes Enable Highly Active Electrocatalysis of Carbon Dioxide Reduction. *Nat. Commun.* **2019**, *10*, 2807.
(34) Meng, F. L.; Zhang, Q.; Duan, Y. X.; Liu, K. H.; Zhang, X. B. Structural Optimization of Metal Oxyhalide for CO_2 Reduction with High Selectivity and Current Density. *Chin. J. Chem.* **2020**, *38* (12), 1752−1756.
(35) Meng, F. L.; Zhang, Q.; Liu, K. H.; Zhang, X. B. Integrated Bismuth Oxide Ultrathin Nanosheets/Carbon Foam Electrode for Highly Selective and Energy-Efficient Electrocatalytic Conversion of CO_2 to HCOOH. *Chem.—Eur. J.* **2020**, *26* (18), 4013−4018.

https://doi.org/10.1021/accountsmr.3c00197
Acc. Mater. Res. 2024, 5, 160−172

(36) Montoya, J. H.; Tsai, C.; Vojvodic, A.; Nørskov, J. K. The Challenge of Electrochemical Ammonia Synthesis: A New Perspective on the Role of Nitrogen Scaling Relations. *ChemSusChem* **2015**, *8* (13), 2180−2186.
(37) Van Kessel, M. a. H. J.; Speth, D. R.; Albertsen, M.; Nielsen, P. H.; Op Den Camp, H. J. M.; Kartal, B.; Jetten, M. S. M.; Lücker, S. Complete Nitrification by a Single Microorganism. *Nature* **2015**, *528* (7583), 555−559.
(38) Bao, D.; Zhang, Q.; Meng, F. L.; Zhong, H. X.; Shi, M. M.; Zhang, Y.; Yan, J. M.; Jiang, Q.; Zhang, X. B. Electrochemical Reduction of N_2 under Ambient Conditions for Artificial N_2 Fixation and Renewable Energy Storage Using N_2/NH_3 Cycle. *Adv. Mater.* **2017**, *29* (3), 1604799.
(39) Xu, L.; Jiang, Q. Q.; Xiao, Z. H.; Li, X. Y.; Huo, J.; Wang, S. Y.; Dai, L. M. Plasma-Engraved Co_3O_4 Nanosheets with Oxygen Vacancies and High Surface Area for the Oxygen Evolution Reaction. *Angew. Chem., Int. Ed.* **2016**, *55* (17), 5277−5281.
(40) Wang, Y.; Shi, M. M.; Bao, D.; Meng, F. L.; Zhang, Q.; Zhou, Y. T.; Liu, K. H.; Zhang, Y.; Wang, J. Z.; Chen, Z. W.; Liu, D. P.; Jiang, Z.; Luo, M.; Gu, L.; Zhang, Q. H.; Cao, X. Z.; Yao, Y.; Shao, M. H.; Zhang, Y.; Zhang, X. B.; Chen, J. G.; Yan, J. M.; Jiang, Q. Generating Defect-Rich Bismuth for Enhancing the Rate of Nitrogen Electroreduction to Ammonia. *Angew. Chem., Int. Ed.* **2019**, *58* (28), 9464−9469.
(41) Ren, Z. H.; Shi, K. G.; Feng, X. F. Elucidating the Intrinsic Activity and Selectivity of Cu for Nitrate Electroreduction. *ACS Energy Lett.* **2023**, *8* (9), 3658−3665.
(42) Chen, C.; Zhu, X. R.; Wen, X. J.; Zhou, Y. Y.; Zhou, L.; Li, H.; Tao, L.; Li, Q. L.; Du, S. Q.; Liu, T. T.; Yan, D. F.; Xie, C.; Zou, Y. Q.; Wang, Y. Y.; Chen, R.; Huo, J.; Li, Y. F.; Cheng, J.; Su, H.; Zhao, X.; Cheng, W. R.; Liu, Q. H.; Lin, H. Z.; Luo, J.; Chen, J.; Dong, M. D.; Cheng, K.; Li, C. G.; Wang, S. Y. Coupling N_2 and CO_2 in H_2O to Synthesize Urea under Ambient Conditions. *Nat. Chem.* **2020**, *12* (8), 717−724.
(43) Zhou, N.; Wang, Z.; Zhang, N.; Bao, D.; Zhong, H. X.; Zhang, X. B. Potential-Induced Synthesis and Structural Identification of Oxide-Derived Cu Electrocatalysts for Selective Nitrate Reduction to Ammonia. *ACS Catal.* **2023**, *13* (11), 7529−7537.
(44) Zhou, N.; Wang, J. Z.; Zhang, N.; Wang, Z.; Wang, H. G.; Huang, G.; Bao, D.; Zhong, H. X.; Zhang, X. B. Defect-Rich Cu@CuTCNQ Composites for Enhanced Electrocatalytic Nitrate Reduction to Ammonia. *Chin. J. Catal.* **2023**, *50*, 324−333.
(45) Wu, J. B.; Yang, H. Platinum-Based Oxygen Reduction Electrocatalysts. *Acc. Chem. Res.* **2013**, *46* (8), 1848−1857.
(46) Liu, R.; Wu, D.; Feng, X.; Müllen, K. Nitrogen-Doped Ordered Mesoporous Graphitic Arrays with High Electrocatalytic Activity for Oxygen Reduction. *Angew. Chem., Int. Ed.* **2010**, *49* (14), 2565−2569.
(47) Zhong, H. X.; Wang, J.; Zhang, Y. W.; Xu, W. L.; Xing, W.; Xu, D.; Zhang, Y. F.; Zhang, X. B. ZIF-8 Derived Graphene-Based Nitrogen-Doped Porous Carbon Sheets as Highly Efficient and Durable Oxygen Reduction Electrocatalysts. *Angew. Chem., Int. Ed.* **2014**, *53* (51), 14235−14239.
(48) Jiang, S.; Zhu, C. Z.; Dong, S. J. Cobalt and Nitrogen-Cofunctionalized Graphene as a Durable Non-Precious Metal Catalyst with Enhanced ORR Activity. *J. Mater. Chem. A* **2013**, *1* (11), 3593−3599.
(49) Ramaswamy, N.; Tylus, U.; Jia, Q.; Mukerjee, S. Activity Descriptor Identification for Oxygen Reduction on Nonprecious Electrocatalysts: Linking Surface Science to Coordination Chemistry. *J. Am. Chem. Soc.* **2013**, *135* (41), 15443−15449.
(50) Wang, Z. L.; Xu, D.; Zhong, H. X.; Wang, J.; Meng, F. L.; Zhang, X. B. Gelatin-Derived Sustainable Carbon-Based Functional Materials for Energy Conversion and Storage with Controllability of Structure and Component. *Sci. Adv.* **2015**, *1* (1), No. e1400035.
(51) Liu, S. W.; Li, C. C.; Zachman, M. J.; Zeng, Y. C.; Yu, H. R.; Li, B. Y.; Wang, M. Y.; Braaten, J.; Liu, J. W.; Meyer, H. M.; Lucero, M.; Kropf, A. J.; Alp, E. E.; Gong, Q.; Shi, Q. R.; Feng, Z. X.; Xu, H.; Wang, G. F.; Myers, D. J.; Xie, J.; Cullen, D. A.; Litster, S.; Wu, G. Atomically Dispersed Iron Sites with a Nitrogen-Carbon Coating as Highly Active and Durable Oxygen Reduction Catalysts for Fuel Cells. *Nat. Energy* **2022**, *7* (7), 652−663.
(52) Li, J. K.; Sougrati, M. T.; Zitolo, A.; Ablett, J. M.; Oğuz, I. C.; Mineva, T.; Matanovic, I.; Atanassov, P.; Huang, Y.; Zenyuk, I.; Di Cicco, A.; Kumar, K.; Dubau, L.; Maillard, F.; Dražić, G.; Jaouen, F. Identification of Durable and Non-Durable Fenx Sites in Fe-N-C Materials for Proton Exchange Membrane Fuel Cells. *Nat. Catal.* **2021**, *4* (1), 10−19.
(53) Meng, F. L.; Zhong, H. X.; Yan, J. M.; Zhang, X. B. Iron-Chelated Hydrogel-Derived Bifunctional Oxygen Electrocatalyst for High-Performance Rechargeable Zn-Air Batteries. *Nano Res.* **2017**, *10* (12), 4436−4447.
(54) Meng, F. L.; Wang, Z. L.; Zhong, H. X.; Wang, J.; Yan, J. M.; Zhang, X. B. Reactive Multifunctional Template-Induced Preparation of Fe-N-Doped Mesoporous Carbon Microspheres Towards Highly Efficient Electrocatalysts for Oxygen Reduction. *Adv. Mater.* **2016**, *28* (36), 7948−7955.
(55) Zhong, H. X.; Li, K.; Zhang, Q.; Wang, J.; Meng, F. L.; Wu, Z. J.; Yan, J. M.; Zhang, X. B. In Situ Anchoring of Co_9S_8 Nanoparticles on N and S Co-Doped Porous Carbon Tube as Bifunctional Oxygen Electrocatalysts. *NPG Asia Mater.* **2016**, *8* (9), No. e308.
(56) Zhong, H. X.; Wang, J.; Zhang, Q.; Meng, F. L.; Bao, D.; Liu, T.; Yang, X. Y.; Chang, Z. W.; Yan, J. M.; Zhang, X. B. In Situ Coupling Fem (M = Ni, Co) with Nitrogen-Doped Porous Carbon toward Highly Efficient Trifunctional Electrocatalyst for Overall Water Splitting and Rechargeable Zn-Air Battery. *Adv. Sustain. Syst.* **2017**, *1* (6), 1700020.
(57) Meng, F. L.; Zhong, H. X.; Bao, D.; Yan, J. M.; Zhang, X. B. In Situ Coupling of Strung Co_4N and Intertwined N-C Fibers toward Free-Standing Bifunctional Cathode for Robust, Efficient, and Flexible Zn-Air Batteries. *J. Am. Chem. Soc.* **2016**, *138* (32), 10226−10231.
(58) Zhong, H. X.; Ghorbani-Asl, M.; Ly, K. H.; Zhang, J. C.; Ge, J.; Wang, M. C.; Liao, Z. Q.; Makarov, D.; Zschech, E.; Brunner, E.; Weidinger, I. M.; Zhang, J.; Krasheninnikov, A. V.; Kaskel, S.; Dong, R. H.; Feng, X. L. Synergistic Electroreduction of Carbon Dioxide to Carbon Monoxide on Bimetallic Layered Conjugated Metal-Organic Frameworks. *Nat. Commun.* **2020**, *11* (1), 1721.
(59) Zhong, H. X.; Wang, M. C.; Ghorbani-Asl, M.; Zhang, J. C.; Ly, K. H.; Liao, Z. Q.; Chen, G. B.; Wei, Y. D.; Biswal, B. P.; Zschech, E.; Weidinger, I. M.; Krasheninnikov, A. V.; Dong, R. H.; Feng, X. L. Boosting the Electrocatalytic Conversion of Nitrogen to Ammonia on Metal-Phthalocyanine-Based Two-Dimensional Conjugated Covalent Organic Frameworks. *J. Am. Chem. Soc.* **2021**, *143* (47), 19992−20000.
(60) Hao, Q.; Zhong, H. X.; Wang, J. Z.; Liu, K. H.; Yan, J. M.; Ren, Z. H.; Zhou, N.; Zhao, X.; Zhang, H.; Liu, D. X.; Liu, X.; Chen, L. W.; Luo, J.; Zhang, X. B. Nickel Dual-Atom Sites for Electrochemical Carbon Dioxide Reduction. *Nat. Synth.* **2022**, *1* (9), 719−728.

https://doi.org/10.1021/accountsmr.3c00197
Acc. Mater. Res. 2024, 5, 160−172